Development of a Spatial Hydrologic Soil Map Using Spectral Reflectance Band Recognition and a Multiple-Output Artificial Neural Network Model

Khamis Naba Sayl[1,3], Haitham Abdulmohsin Afan[1], Nur Shazwani Muhammad[1], Ahmed ElShafie[2]

[1]Department of Civil and Structural Engineering, Faculty of Engineering and Built Environment, Universiti Kebangsaan Malaysia, 43600 UKM Bangi, Selangor Darul Ehsan, Malaysia
[2]Department of Civil Engineering, Faculty of Engineering, University of Malaya, 50603 Kuala Lumpur, Malaysia
[3]Department of Dams and Water Resources, Engineering College, University of Anbar, Ramadi, Iraq

Correspondence to: Nur Shazwani Muhammad (shazwani.muhammad@ukm.edu.my)

Abstract. Soil type is important in any civil engineering project. Thorough and comprehensive information on soils in both the spatial and temporal domains can assist in sustainable hydrological, environmental and agricultural development. Conventional soil sampling and laboratory analysis are generally time-consuming, costly and limited in their ability to retrieve the temporal and spatial variability, especially in large areas. Remote sensing is able to provide meaningful data, including soil properties, on several spatial scales using spectral reflectance. In this study, a multiple-output artificial neural network model was integrated with geographic information system, remote sensing and survey data to determine the distributions of hydrologic soil groups in the Horan Valley in the Western Desert of Iraq. The model performance was evaluated using seven performance criteria along with the hydrologic soil groups developed by the United States Geological Survey (USGS). On the basis of the performance criteria, the model performed best for predicting the spatial distribution of clay soil, and the predicted soil types agreed well with the soil classifications of the USGS. Most of the samples were categorized as sandy loam, whereas one sample was categorized as loamy sand. The proposed method is reliable for predicting the hydrological soil groups in a study area.

1 Introduction

Spatial and temporal information on soil type is important in any civil engineering project in order to ensure sustainable hydrological, environmental and agricultural development. Hydrological processes, including surface runoff and infiltration, depend on the soil texture. Therefore, soil type is important in determining the potential volume of surface runoff and selecting the best type and location of water-harvesting structures (Jasrotia et al. 2009).

Currently, the Soil Conservation Service (SCS) method is used widely in many types of studies to estimate the surface runoff from a certain rainfall event (Senay and Verdin 2004; Winnaar et al. 2007; Tyagi et al. 2008; Elewa and Qaddah 2011). This method is based on the runoff curve number (CN), which is derived from the soil texture and land cover, where soil type is classified into several subcategories. The United States Geological Survey (USGS) has divided hydrologic soil groups into four classes. Runoff can be estimated using CN from the rainfall amount (Senay and Verdin 2004). Many hydrological models use CN as input to estimate storm runoff, such as the Soil and Water Assessment Tool (SWAT) (Neitsch et al. 2011), Environmental Policy Integrated Climate (EPIC) model (Wang et al. 2012) and Agricultural Non-Point Source Pollution (AGNPS) model (Young et al. 1987).

The identification of soil type based on laboratory testing is considered to be a traditional method, and it is time-consuming and costly. Remote sensing (RS) represents one of the best alternatives; it is an accessible method that can be utilized to provide valuable information related to site evaluation, including site monitoring and soil investigation. Furthermore, this information can be easily analysed and integrated for site design, environmental impact assessment and planning for construction activities. RS is capable of providing soil information in a spatial form, which is very significant in the prediction of soil properties based on various bands of the electromagnetic spectrum.

The spectral reflectance characteristics of soils are a function of several important characteristics (Lacoste et al. 2014; Martin et al. 2014; Wulf et al. 2014). The chemical and physical properties of materials define their spectral reflectance and emittance spectra, which can be used to identify them. Spectral reflectance refers to the ratio of radiant energy reflected to the incident energy on a body (Sims and Gamon 2002).

The soil reflectance data can be measured under laboratory conditions (i.e. proximal sensing) or in the field (i.e. RS). The process of measuring soil reflectance using the proximal sensing method suffers from several problems, such as variations in view angle, illumination, soil surface roughness and exact ground position. The effectiveness of RS depends on the atmospheric conditions and the strength of the signal in the study area. The relationship between soil type and reflectance is represented by ~~five specific~~ soil spectral reflectance curves developed by Stoner and Baumgardner (1981). These curves provide important information about the presence or absence of organic matter and iron along with absorption, which indicate different soil textures.

Over the last few decades, several studies have demonstrated that some soil characteristics can be determined using laboratory spectral analysis (Salisbury and D’Aria 1992; Chang and Laird 2002; Nanni and Demattê 2006; Minasny and McBratney 2008). Odeh and McBratney (2000) employed a multi-variate prediction model based on advanced very-high-resolution radiometer (AVHRR) to map a large area of clay. The correlations between the image data and laboratory analysis of SPOT, airborne spectroscopy and Landsat TM were used to determine different classes of soil textures (Proctor et al. 2000). The various types of soil were classified with accuracy from 50% up to 100%using these correlations. Such a poor correlation cannot be used to establish the relationship between soil texture and reflectance. Chang and Islam (2000) used multi-temporal remotely sensed brightness temperature and soil moisture map to infer the physical properties of soils. Two artificial neural networks (ANNs) were constructed based on the physical linkages among the space–time distributions of brightness temperature, soil moisture and soil media properties.

Apan et al. (2002) used a primary component image of the Advanced Spaceborne Thermal Emission and Reflection (ASTER) radiometer (bands 2 and 8) to determine classes of soil textures. They found that the absorption characteristics of soil can be used to differentiate quartz and clay soils on the map. Chabrillat et al. (2002) found that a short-wave with bands 5 and 6 of ASTER can detect clay soil, and the quartz index can be captured by thermal bands 10–14. Other studies showed that the short and thermal waves of ASTER can detect sandy and dark clayey soils, although the results differed depending on the presence of organic substances (Salisbury and D'Aria 1992; Breunig and Galvão 2008).

Soil reflectance is a complex phenomenon. It is difficult to predict the soil reflectance properties using physical models and theories owing to the possibility of quantitative conversion of the reflectance spectrum of the multi-mineral surface to the actual mineral abundances (Clark and Roush 1984). In addition, the theoretical results do not usually agree with reality and are not valid for the assessment of soil properties (Dewitte et al. 2012; Wulf et al. 2014). Thus, we need to establish a method that is able to reveal the complex relationships between reflectance and soil properties, especially in large areas.

This study presents a methodology for the recognition of soil textures. This methodology integrates ANN, Geographic Information System (GIS) and RS. Artificial intelligence (AI) improved the viewpoints of digital soil mapping, and the integration of GIS helps to achieve complete area coverage. The proposed methodology is extremely useful in large areas, where data are scarce and have limited availability. The applicability of this method is tested to a study area located in the Western Desert of Iraq.

2 Study Area

Wadi Horan, which is one of the largest valleys in the Western Desert of Iraq, was selected as the study area. It is located in the southern part of the Euphrates ~~River, and its geographic coordinates range from 32° 10′ 44″ to 34° 11′ 00″ N (latitude) and from 39° 20′ 00″ to 42° 30′ 00″ E (longitude),~~ as shown in Fig. 1. The total catchment area is 13,370 km^2 ~~(length = 362 km and width = 49.3 km)~~. ~~The perimeter and shape coefficients are 1,307 km and 0.13, respectively~~.

The general climate is arid, which means that the area is dry in summer and cool in winter. There is a significant variation in daily temperature (i.e. approximately 36°C). These conditions cause the land surface to heat up during the day and cool during the night, which breaks the land surface into fragments and blocks. The high annual amount of evaporation (3,200 mm), low average annual rainfall (115 mm) and high infiltration rate (3.25 mm/h) result in water scarcity in the region.

The study area is flat, and the elevation increases moving westward. The average topographic incline from east to west is 5 m/km, and the elevations of the highest and lowest points in the area are 987 and 77 m above sea level, respectively. The main landscape is a plateau characterized by dense valleys. Some of the valleys are canyon-like with lengths of a few tens of kilometres, and others are few hundred kilometres in length.

The major plateau of the catchment is rocky. The landform ~~of~~ the study area result~~s~~ from the complex interactions among the structure, lithology and climate. The lithologic column of the uncovered rocks in the Western Desert consists of limestone, dolomitic limestone, marl, dolomite, claystone, sandstone and phosphorite with rare gypsum (Sissakian et al. 2011). In general, the Western Desert is characterized by low rainfall, thick soil cover and the absence of vegetation. The study area includes some positive topographic features such as canyons, cliffs, depressions and major valleys. Depressions, either erosional or solution in form, are another characteristic feature. The depressions have different sizes and shapes, primarily including circular, oval and longitudinal. These features are the most important components in building water-harvesting structures.

3 Methodology

The steps employed to accomplish the objectives of this study were data collection, data preparation and modelling, as shown in Fig. 2. ~~The details regarding the methodology are provided in the following paragraphs.~~

~~S~~atellite images of the study area were collected from Landsat 8 in August 2014. These images were imported into the ERDAS Imagine software for geometric correction using WGS 84/UTM zone 38 projection. Subsequently, unsupervised classification was carried out in the study area. Results from the unsupervised classification provide a good depiction of some spectral classes and categorized these classes on the basis of the ranges of the image value. Therefore, unsupervised classification is a useful task and includes the preparation of a primitive map for reconnaissance, soil survey, to identify locations for soil sampling to reduce the effort time and cost. An easily accessible flat surface consisting of bare soil and containing all types of soil with an area of $70 \times 70\ km^2$ was selected based on unsupervised classification of the entire study area. The primitive map was produced by colour-coding each individual pixel to represent the class into which it was assigned by the classification algorithm. This map is a useful way to present the information extracted by the classification process. In addition, the use of the primitive map will reduce the error in pixel vegetation cover by more than 20% along with the errors associated with the spectral signatures urban areas, water, roads, slope, soil roughness, locations and topography for each point selected. All these specifications are recommended for accurate classification (Bartholomeus et al. 2008). Thus, the unsupervised classification is an essential step in preparing the primitive maps, conducting the soil survey and collecting the soil sample.

In the next phase, soil sampling locations were pre-selected based on the unsupervised classification thematic map. Twenty-five sampling locations throughout the study area were selected using a GPS instrument based on certain criteria. Subsequently, the soil samples were brought to the laboratory, and sieve analysis was carried out to estimate the percentages of sand, clay and silt in each sample. The particle size analysis of a soil sample involves determining percentage by weight of particles within different size ranges. The sieve analysis data were divided into training and validation sets containing 19 and 6 samples, respectively.

Subsequently, site investigations were carried out. A satellite image from Landsat 8 was used to determine the spectral reflectance of each location using ERDAS software based on the actual locations, which were determined using a GPS device. The spectral reflectance for the visible, near infrared and short wave infrared, which are represented by nine bands, were recorded for each location, whereas two thermal infrared bands were reduced.

After the laboratory work and site investigations were complete, a sensitivity analysis was carried out to examine the relationship between bands and soil texture. The results were used to develop a database for soil type based on spectral reflectance using the radial basis neural network model. The results of this model for each type of soil have been evaluated based on seven criteria [i.e. root mean square error (RMSE), normalized root mean square error (NRMSE), mean absolute error (MAE), normalized mean absolute error (NMAE), minimum absolute error, maximum absolute error and correlation coefficient (*r*)]. The results of the radial basis neural network were verified using the hydrologic soil group classification developed by USGS. The soil classifications were then manipulated within ArcGIS 10.2 using the spatial analyst model to generate a digital map of hydrologic soil groups for the entire study area. Figure 3 summarises the methodology used in this study, including the strategies for data collection, data manipulation and modelling.

4 Results and Discussion

The selection of sampling locations is based on certain criteria which have been mentioned previously in the methodology to reduce the errors associated with spectral signatures and accurately estimate soil characteristics; thus, a better unsupervised classification was performed, as shown in Fig. 4. Figure 4 shows ten classes of land cover (vegetation and different types of soil), and each class is given a specific colour. The soil texture for each position is given in detail in Table 1. The spectral reflectance was recorded for each position using ERDAS software. Nine bands were used, as shown in Table 1.

A sensitivity analysis was carried out to validate the relationship between soil type and spectral reflectance, as shown in Fig. 5. Soil type could not be detected by band 2 (wavelength (0.45–0.51) µm). Band 9 (1.36–1.38 µm) and band 7 (2.11–2.29 µm) were the most sensitive to soil type, particularly silt and sand, whereas clayey soil could be detected by band 6 (1.57–1.65 µm), band 1 (0.43–0.45 µm) and band 7. Unfortunately, the spectral reflectance for each range of wavelengths represented by the number of bands has a complex relationship with soil type because all these bands participate in detecting the soil texture, but in different weights because of the mineral content of that soil. Because of the variation in spectral reflectance over bands, a highly accurate model for the estimation of soil type is needed. Therefore, it is important to include all effective bands in the ANN model.

The actual values and values estimated by the ANN model are given in Fig. 6, which shows that sand had a higher percentage than silt and clay. Figure 6 also demonstrates that the values estimated for clay were more accurate than those estimated for sand and silt, and the predicted value for sandy soil was significantly different from the actual value. The overall performance of the ANN model was constant, and the total percentage of output (estimated) was 100%.

The performance of the ANN model for each type of soil was evaluated based on seven criteria, namely RMSE, NRMSE, MAE, NMAE, minimum absolute error, maximum absolute error and *r*. The results indicate that the estimation accuracy varied slightly among the three types of soil. The performance criteria for clay were excellent, and the correlation coefficient for clay was the highest among the three soil types (Table 2). On the basis of the values of NRMSE, NMAE and minimum absolute error, the ANN model generated less error for sand than for silt. In contrast, based on RMSE, MAE, *r* and maximum absolute error, the silt estimation was better than the sand estimation.

Another way to evaluate the performance of the proposed method is through the hydrologic soil groups developed by USGS, as shown in Fig. 7. The blue and red numbers in Fig. 7 are the measured and estimated soil textures, respectively. The estimated values for all sites showed good agreement with the hydrologic soil groups of the USGS. Most of the samples were categorized as sandy loam, whereas sample 1 was categorized as loamy sand. With reference to Fig. 7, there was only a slight difference in the measured and estimated percentages of clay and sand for sample 1. However, both the measured and estimated values are located in hydrologic soil group A. These results indicate that the proposed method is reliable for predicting the soil group of a study area.

The hydrologic soil map was developed for Wadi Horan (Fig. 8). The spectral reflectance of 120 points in different locations were predicted using the ANN model, and the percentages of soil types were determined based on the hydrologic soil classifications of the USGS. Next, the classification data were manipulated within GIS using the spatial analysis model to generate a digital map of hydrologic soil groups. Figure 8 shows the distributions of hydrologic soil types in Wadi Horan Valley.

5 Conclusions

The integration of ANN with GIS, RS data and survey data helps to establish a significant procedure that can be utilized for developing a digital hydrological soil group map. The relationship between spectral reflectance and soil texture was used to predict soil class. This study proposed and evaluated a method to predict a hydrologic soil group for an area by combining an ANN procedure with GIS and RS data. The effectiveness of this methodology was evaluated based on seven performance criteria. The maximum absolute errors (one of the performance criteria) were 7.5, 12.8 and 14.8 for clay, silt and sand content, respectively. Clay soils produced the highest correlation coefficient (0.8565). The overall performance of this methodology was also tested using the hydrologic soil groups developed by USGS; all the samples were predicted to locate in the same hydrologic soil group determined by USGS. Therefore, the proposed methodology performs well for classifying soils. It is also fast, reliable and cost-effective. In addition, this method can be used to generate a database of high quality digital maps for authorities and stake holders.

Author contribution

K. N. Sayl collected the data, designed the methodology and perform the experiments. H. A. Afan and A. ElShafie assist in the development of artificial neural network codes. N. S. Muhammad monitors the research progress and prepared the manuscript with contributions from all co-authors.

Acknowledgement

The authors would like to thank Universiti Kebangsaan Malaysia for their financial support through the Geran Galakan Penyelidik Muda, grant number GGPM-2014-046.

References

Apan, A., Kelly, R., Jensen, T., Butler, D., Strong, W., and Basnet, B.: Spectral discrimination and separability analysis of agricultural crops and soil attributes using ASTER imagery, in: 11th Australasian Remote Sensing and Photogrammetry Conference, 396–411, 2002 .

Bartholomeus, H. M., Schaepman, M. E., Kooistra, L., Stevens, A., Hoogmoed, W. B., and Spaargaren, O. S. P.: Spectral reflectance based indices for soil organic carbon quantification, Geoderma, 145, 28–36, doi: 10.1016/j.geoderma.2008.01.010, 2008.

Breunig, F., Galvão, L., Formaggio, A. R.: Detection of sandy soil surfaces using ASTER-derived reflectance, emissivity and elevation data: potential for the identification of land degradation, Int. J. Remote Sens., 29, 1833–1840, 2008.

Chabrillat, S., Goetz, A., Krosley, L., and Olsen, H.: Use of hyperspectral images in the identification and mapping of expansive clay soils and the role of spatial resolution, Remote Sens. Environ., 82, 431–445, 2002.

Chang, C., and Laird, D.: Near-infrared reflectance spectroscopic analysis of soil C and N, Soil Sci., 167, 110–116, 2002.

Chang, D. H., and Islam, S.: Estimation of soil physical properties using remote sensing and artificial neural network, Remote Sens. Environ., 74, 534–544, doi: 10.1016/s0034-4257(00)00144-9, 2000.

Clark, R., and Roush, T.: Reflectance spectroscopy: Quantitative analysis techniques for remote sensing applications, J. Geophys. Res.-Sol. Ea., 89, 6329–6340, 1984.

De Winnaar, G., Jewitt, G., and Horan, M.: A GIS-based approach for identifying potential runoff harvesting sites in the Thukela River basin, South Africa, Phys. Chem. Earth Pt. A/B/C, 32, 1058–1067, 2007.

Dewitte, O., Jones, A., Elbelrhiti, H., Horion, S., and Montanarella, L.: Satellite remote sensing for soil mapping in Africa: An overview, Prog. Phys. Geog., 0309133312446981, 2012.

Elewa, H. H., and Qaddah, A. A.: Groundwater potentiality mapping in the Sinai Peninsula, Egypt, using remote sensing and GIS-watershed-based modeling. Hydrogeol. J., 19, 613–628, doi: 10.1007/s10040-011-0703-8, 2011.

Jasrotia, A. S., Majhi, A., and Singh, S.: Water balance approach for rainwater harvesting using remote sensing and GIS techniques, Jammu Himalaya, India. Water Resour. Manag., 23, 3035–3055, doi: 10.1007/s11269-009-9422-5, 2000.

King, C., Baghdadi, N., Lecomte, V., and Cerdan, O.: The application of remote-sensing data to monitoring and modelling of soil erosion, Catena, 62, 79–93, 2005.

Lacoste, M., Minasny, B., McBratney, A., Michot, D., Viaud, V., and Walter, C.: High resolution 3D mapping of soil organic carbon in a heterogeneous agricultural landscape, Geoderma, 213, 296–311, 2014.

Martin, M., Orton, T., Lacarce, E., Meersmans, J., Saby, N. P. A., Paroissien, J. B., Jolivet, C., Boulonne, L., and Arrouays, D.: Evaluation of modelling approaches for predicting the spatial distribution of soil organic carbon stocks at the national scale, Geoderma, 223, 97–107, 2014.

Minasny, B., and McBratney, A.: Regression rules as a tool for predicting soil properties from infrared reflectance spectroscopy, Chemometr. Intell. Lab., 94, 72–79, 2008.

Nanni, M., and Demattê, J.: Spectral reflectance methodology in comparison to traditional soil analysis, Soil Sci. Soc. Am. J., 70, 393–407, 2006.

Neitsch, S., Arnold, J., Kiniry, J., and Williams, J.: Soil & water assessment tool theoretical documentation version 2009. Texas Water. Resour. Inst., 1–647, 2011.

Odeh, I., and McBratney, A.: Using AVHRR images for spatial prediction of clay content in the lower Namoi Valley of eastern Australia, Geoderma, 97, 237–254, 2000.

Proctor, C., Baker, A., Barnes, W., and Gilmour, M.: A thousand year speleothem proxy record of North Atlantic climate from Scotland, Clim. Dynam., 16, 815–820, 2000.

Salisbury, J., and D'Aria, D.: Infrared (8–14 μm) remote sensing of soil particle size, Remote Sens. Environ., 42, 157–165, 1992.

Senay, G., and Verdin, J.: Developing index maps of water-harvest potential in Africa, Appl. Eng. Agric., 20, 789, 2004.

Sims, D., and Gamon, J.: Relationships between leaf pigment content and spectral reflectance across a wide range of species, leaf structures and developmental stages, Remote Sens. Environ., 81, 337–354, 2002.

Sissakian, V., Ahad, A., and Hamid, A.: Geological hazards in Iraq, classification and geographical distribution, Iraqi Bulletin of Geology and Mining, 7, 1–28, 2011.

Stoner, E., and Baumgardner, M.: Characteristic variations in reflectance of surface soils, Soil Sci. Soc. Am. J., 45, 1161–1165, 1981.

Tyagi, J., Mishra, S., Singh, R., and Singh, V.: SCS-CN based time-distributed sediment yield model, J. Hydrol., 352, 388–403, 2008.

Wang, X., Williams, J. R., Gassman, P. W., Baffaut, C., Izaurralde, R. C., Jeong, J., and Kiniry, J. R.: EPIC and APEX: Model use, calibration, and validation, Trans. ASABE, 55, 1447–1462, doi: 10.13031/2013.42253, 2012.

Wulf, H., Mulder, T., Schaepman, M., Keller, A., and Jörg, P.: Remote sensing of soils, Zurich, Switzerland, 71, 2014.

Young, R., Onstad, C., Bosch, D., and Anderson, W.: AGNPS, Agricultural Non-Point-Source Pollution Model: a watershed analysis tool. Research report, Agricultural Research Service, Albany, CA (USA). Western Utilization Research and Development Div., 1987.

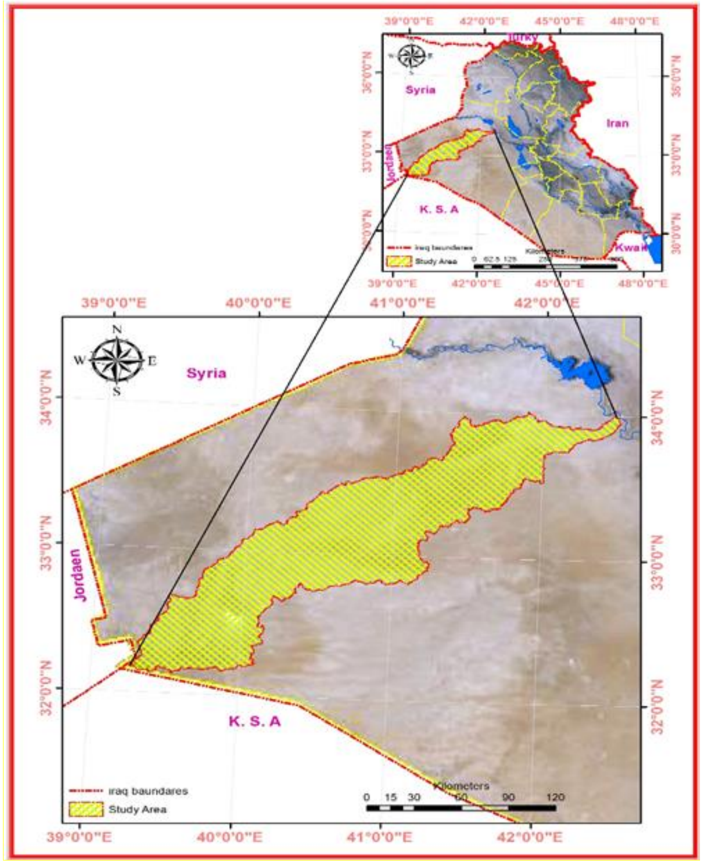

Figure 1: Map of the study area

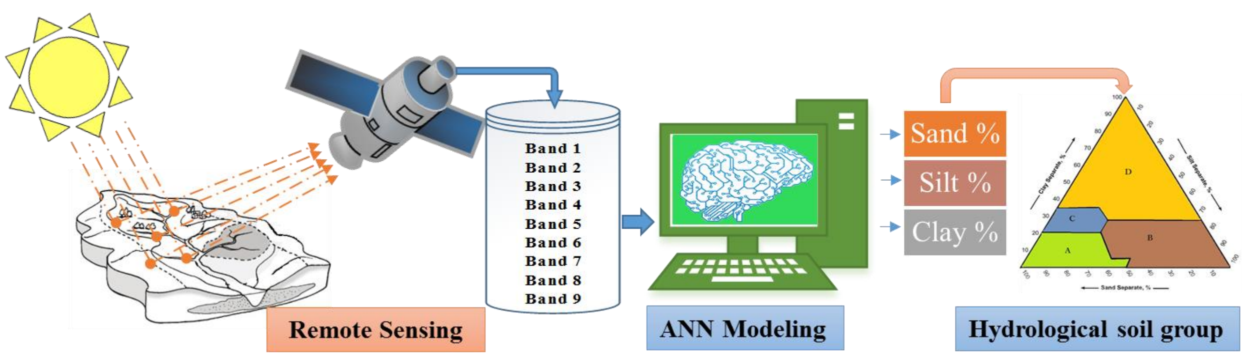

Figure 2: Schematic showing the study methodology

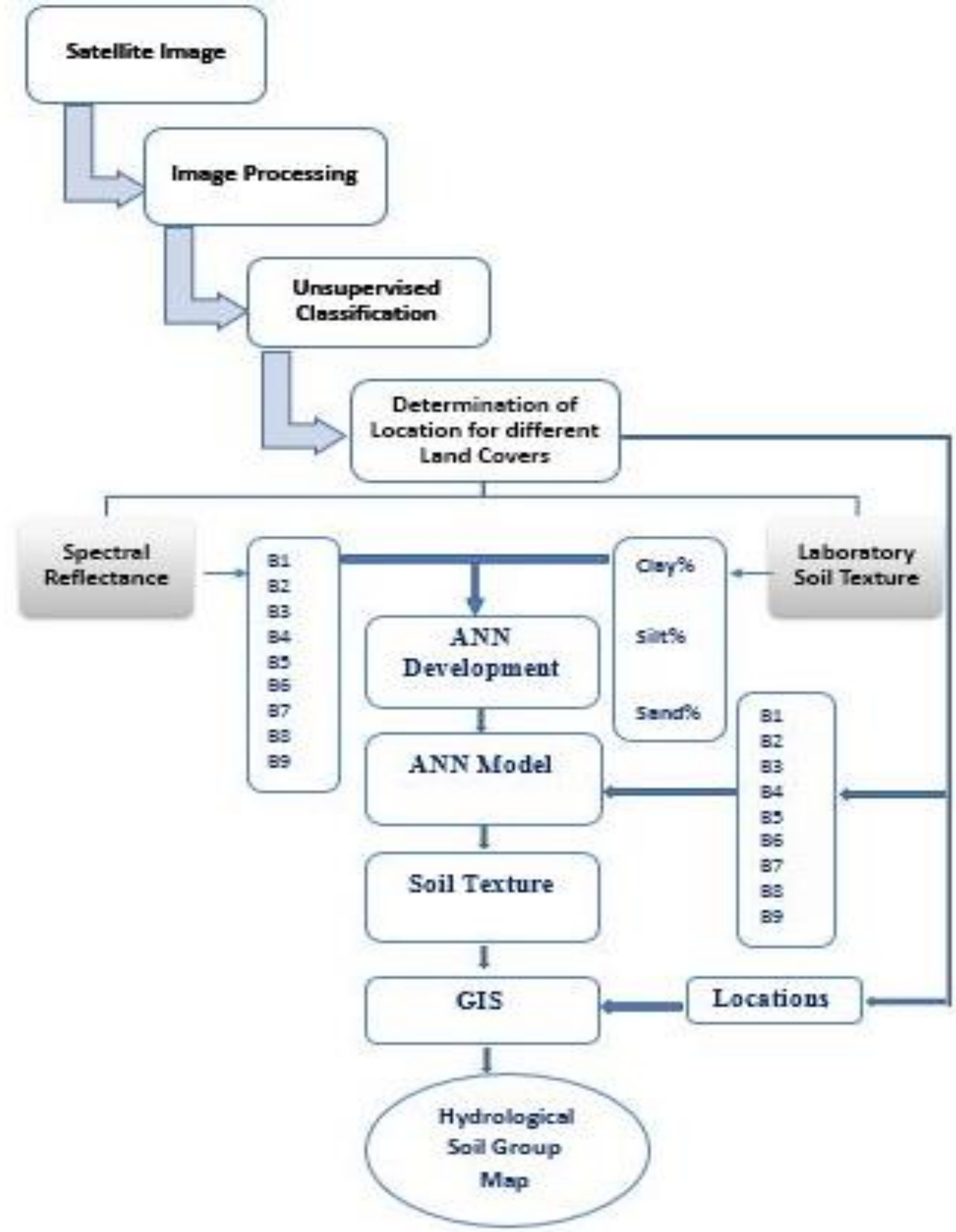

319 **Figure 3: Flowchart showing the proposed methodology**

320

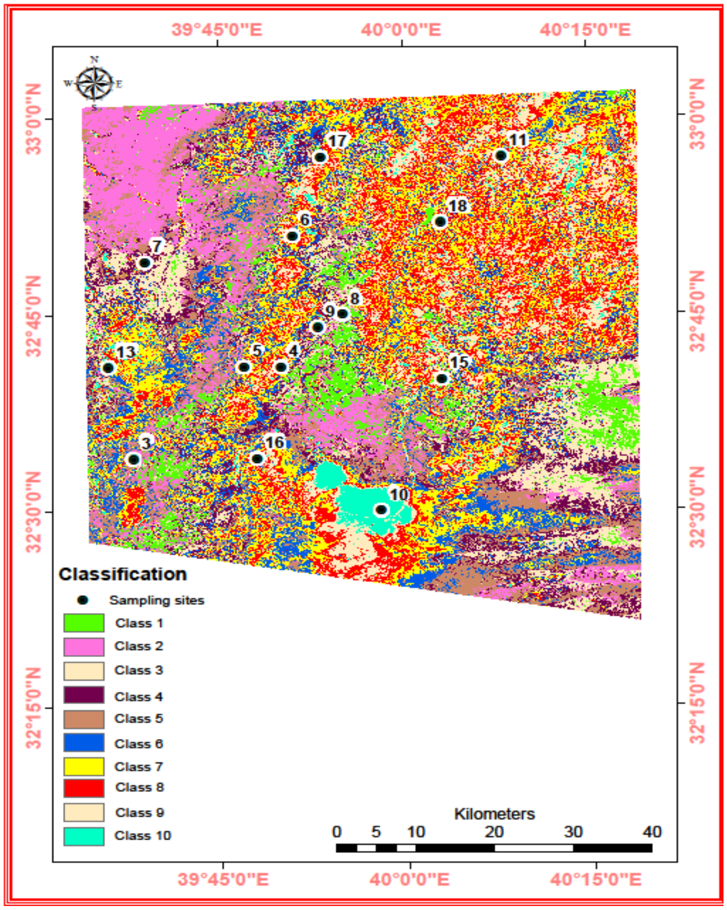

Figure 4: Soil classes of unsupervised classification with samples locations

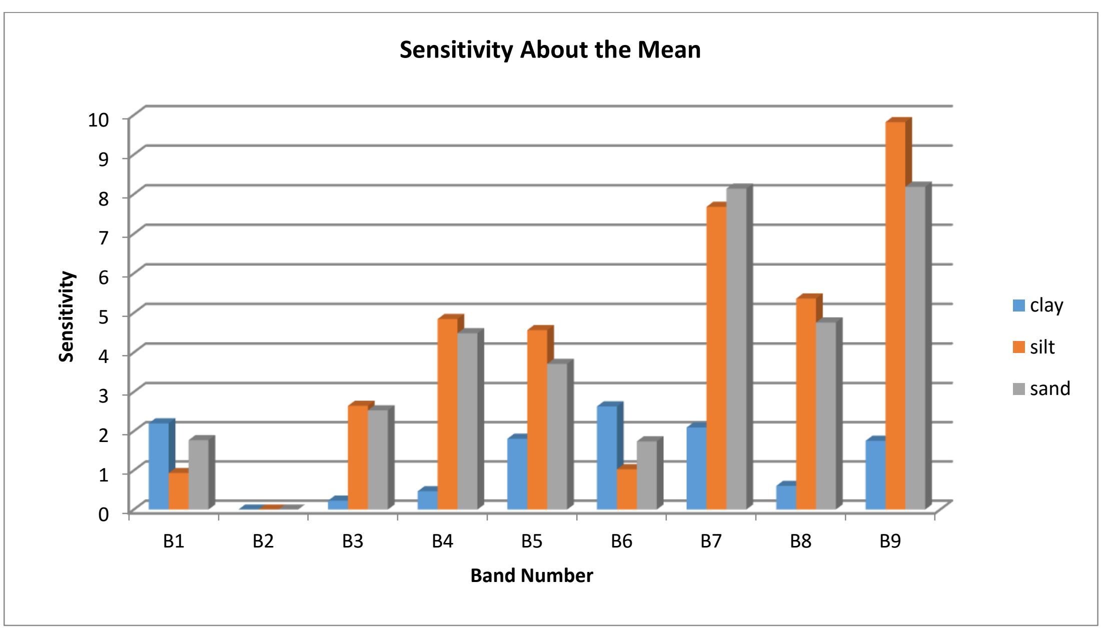

Figure 5: Sensitivities of bands for different soil types

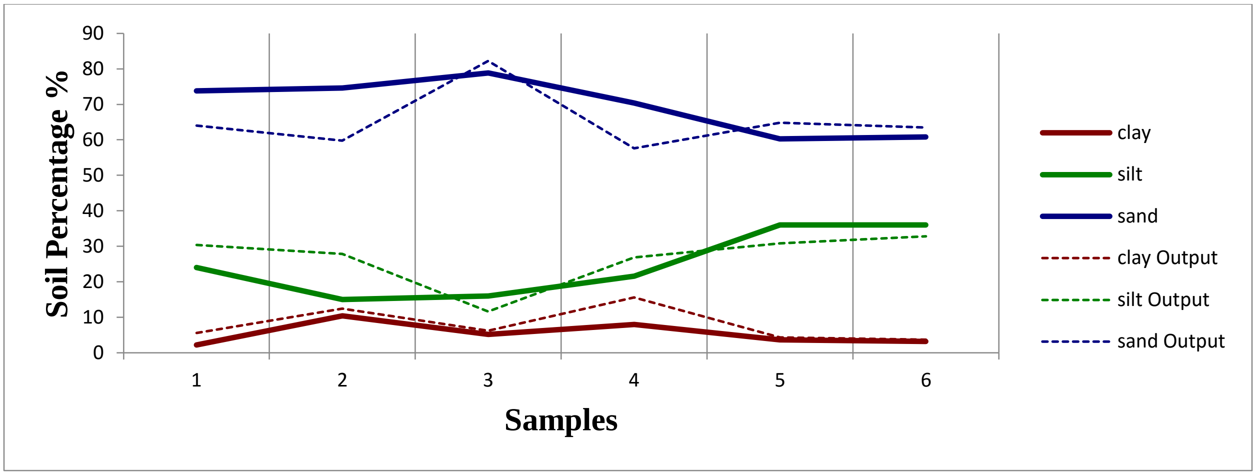

Figure 6: Actual and estimated values of clay, silt, and sand for the tested samples

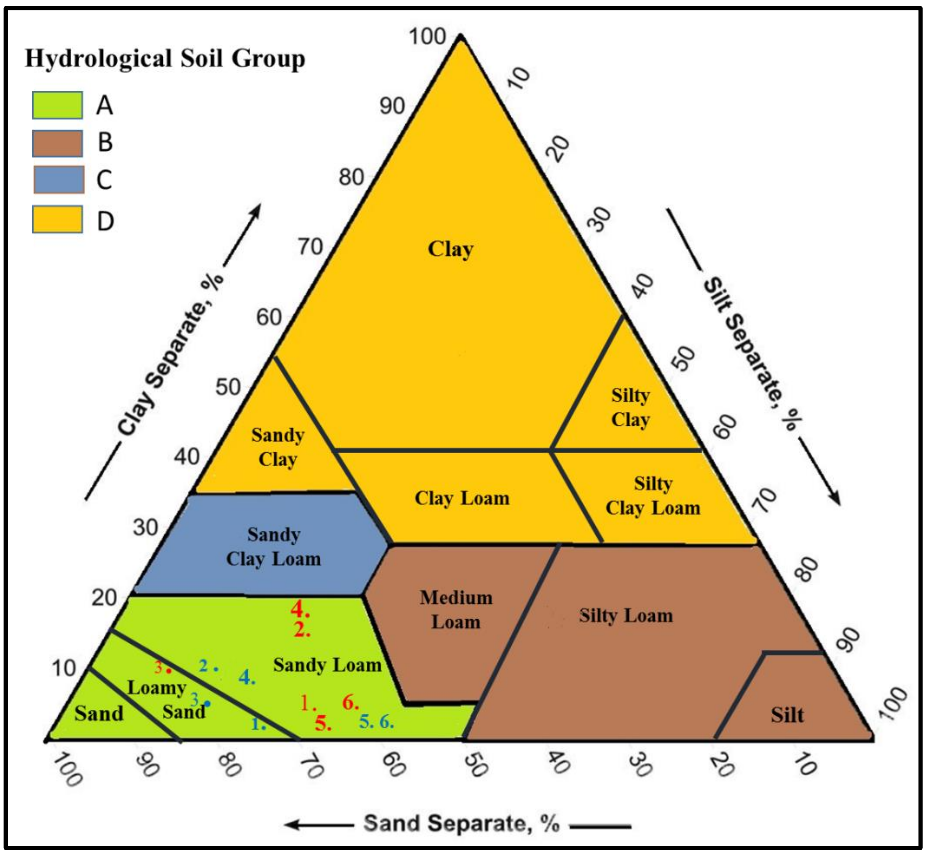

Figure 7: Representations of actual and estimated points on the zones of the hydrologic soil group and the triangle of soil texture

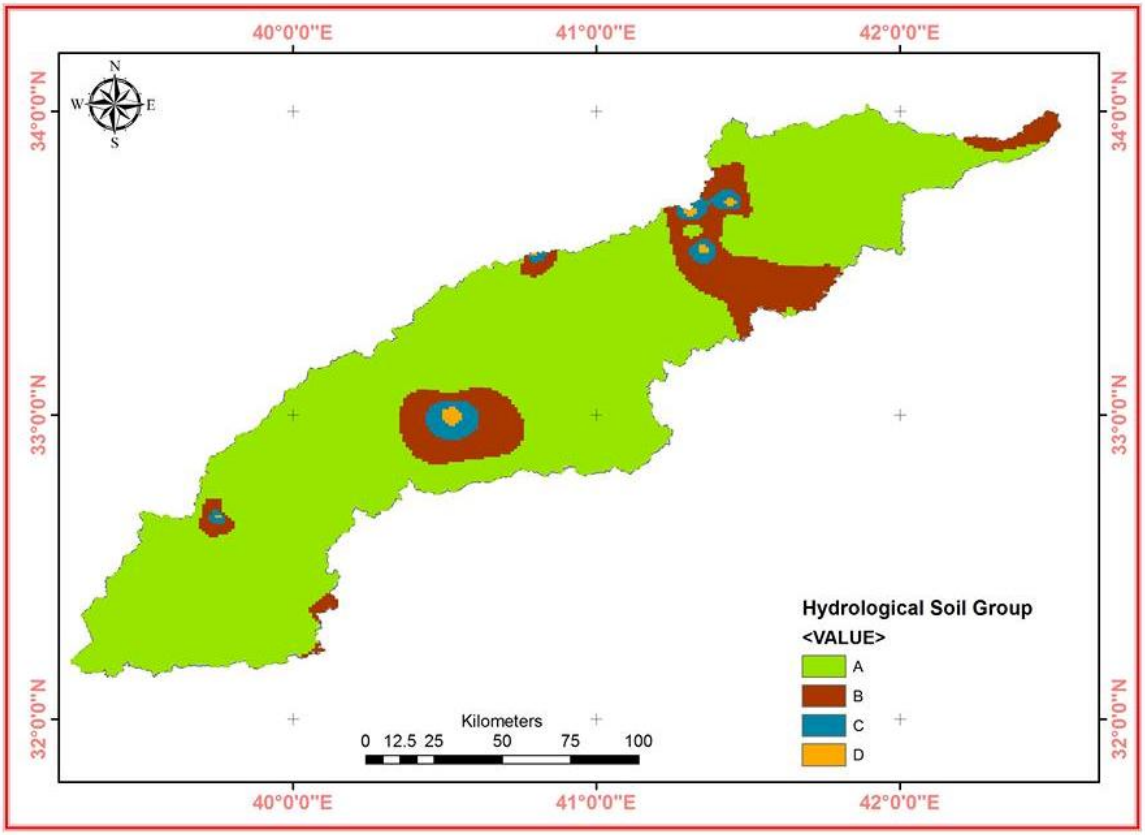

Figure 8: Hydrologic soil group in the Wadi Horan Valley classified using the multiple-output artificial neural network model integrated with the geographic information system, remote sensing and survey data

Table 1: Band number and results of sieve analysis for each point

Point	Band 1	Band 2	Band 3	Band 4	Band 5	Band 6	Band 7	Band 8	Band 9	Clay %	silt %	Sand %
P1	12664	12574	13864	18241	22641	26704	22598	15346	5106	31.2	21.2	47.6
P2	12574	12498	13710	17721	21705	25666	21869	15103	5116	2.2	24.0	73.8
P3	12936	12922	14485	18556	23386	27961	22736	15663	5094	10.4	15.0	74.6
P4	13539	13839	16268	20959	25781	29141	23980	17721	5083	2.0	34.0	64.0
P5	12897	12994	14743	19051	23350	26839	22378	16230	5080	2.6	23.0	74.4
P6	13391	13626	15738	20259	24631	27881	23255	17193	5091	5.2	16.0	78.8
P7	12909	12934	14478	18724	22853	25930	21894	15947	5079	1.0	7.6	91.4
P8	12823	12866	14447	18179	22107	25529	20955	15423	5080	4.0	27.2	68.8
P9	12802	12871	14446	18185	22275	25927	21041	15586	5108	8.0	21.6	70.4
P10	15698	16683	20553	25715	30665	33089	27247	22258	5096	1.2	18.0	80.8
P11	13208	13507	15929	20507	24550	27072	23370	17575	5093	7.2	8.0	84.8
P12	12942	12924	14460	18642	22693	25803	21886	15917	5117	1.2	32.0	66.8
P13	13163	13312	15123	19358	23521	26904	22438	16449	5112	3.7	36.0	60.3
P14	13576	13799	16088	20704	25507	29300	24366	17540	5090	0.0	14.0	86.0
P15	13127	13308	15479	19675	23761	26989	22313	16779	5085	4.0	39.2	56.8
P16	13330	13551	15869	20805	25856	30040	24993	17481	5091	0.6	19.0	80.4
P17	13227	13391	15504	19844	23964	26833	22087	16931	5086	3.2	36.0	60.8
P18	13063	13290	15531	19598	23371	26544	22183	16370	5083	3.2	24.0	72.8
P19	12664	12574	13864	18241	22641	26704	22598	15346	5106	50.2	1.5	48.3
P20	12574	12498	13710	17721	21705	25666	21869	15103	5116	3.6	0.1	96.3
P21	12936	12922	14485	18556	23386	27961	22736	15663	5094	32.0	1.6	66.4
P22	13539	13839	16268	20959	25781	29141	23980	17721	5083	20.5	11.1	68.4
P23	12897	12994	14743	19051	23350	26839	22378	16230	5080	33.5	0.8	65.7
P24	13391	13626	15738	20259	24631	27881	23255	17193	5091	17.0	1.0	82.0
P25	12909	12934	14478	18724	22853	25930	21894	15947	5079	31.2	1.1	67.7

Table 2: Evaluation of the ANN model for each type of soil based on performance criteria

Performance criteria	**clay**	**silt**	**sand**
RMSE	3.5221	6.9521	9.3021
NRMSE	0.1128	0.2201	0.212
MAE	2.5264	6.2112	7.9995
NMAE	0.0809	0.1965	0.1826
Min Abs Error	0.5295	3.2202	2.6906
Max Abs Error	7.5674	12.8539	14.8565
r	0.8565	0.6471	0.4102